Available online at BCREC Website: https://bcrec.undip.ac.id

Bulletin of Chemical Reaction Engineering & Catalysis, 13 (2) 2018, 256-261

Research Article

Feasibility of Macroporous CeO_2 Photocatalysts for Removal of Lead Ions from Water

Takuya Nozaki[1], Ryo Shoji[1*], Yasukazu Kobayashi[2], Kazunori Sato[3]

[1]Department of Chemical Science and Engineering, National Institute of Technology, Tokyo College, Tokyo, Japan
[2]Materials Research Center for Element Strategy, Tokyo Institute of Technology, Kanagawa, Japan
[3]Department of Materials Science and Technology, Nagaoka University of Technology, Niigata, Japan

Received: 21st March 2017; Revised: 31st November 2017; Accepted: 8th December 2017;
Available online: 11st June 2018; Published regularly: 1st August 2018

Abstract

Removal of lead ions from water was conducted by a coupling approach of adsorption and photoelectrodeposition over a macroporous CeO_2 photocatalyst loaded with ZnO. The photocatalyst was prepared by the hard template method and the impregnation method. The various size of silica spheres (0.05-0.4 μm) were used as a template for the photocatalyst, and the highest BET surface area (73.8 m^2/g) was given in the sample prepared with the smallest silica sphere (0.05 μm). In the removal of lead ions, the porous sample showed a large amount of removal of lead ions. In addition, the ZnO loaded catalysts showed a larger amount of removal for lead ions than an unloaded catalyst under the UV light irradiation. In the reaction, since zinc ions were simultaneously dissolved to the solution, it was suggested that this reaction was the ion-exchange reaction between lead ions and zinc ions and was promoted by the UV light irradiation. Copyright © 2018 BCREC Group. All rights reserved

Keywords: CeO_2 photocatalyst; Lead ion removal; Macroporous photocatalyst; Hard template method

How to Cite: Nozaki, T., Shoji, R., Kobayashi, Y., Sato, K. (2018). Feasibility of Macroporous CeO_2 Photocatalysts for Removal of Lead Ions from Water. *Bulletin of Chemical Reaction Engineering & Catalysis*, 13 (2): 256-261 (doi:10.9767/bcrec.13.2.1020.256-261)

Permalink/DOI: https://doi.org/10.9767/bcrec.13.2.1020.256-261

1. Introduction

Heavy metal ions are toxic and often discharged into public water environments by industrial processes, such as factory effluents. Heavy metal ions cause serious damage to the human body and the environment because of the high toxicity [1]. According to the environmental criteria suggested by WHO, the concentrations of heavy metals in water are required to be decreased down to the ppb level [2]. Commonly, many effective techniques have been proposed for heavy metal ion removal from water, such as chemical precipitations using hydroxide, sulfide and chelating agents, ion exchange processes, adsorption and so on [1,3]. Among them, adsorption seems to be the most attractive approach due to its recovery merit and easy handling. However, it is difficult to remove the total metal ions by only adsorption due to an accompanying desorption process. Many studies on the removal of heavy metal ions by photocatalysts have already been conducted [4,5]. These methods mainly remove heavy metal ions by using both adsorption and photoelectrodeposition at the same time. A larger amount of lead ions can be removed by both methods than by the adsorption method only. Generally, photocatalytic activity can be increased by good crystallinity, large specific sur-

---

* Corresponding Author.
E-mail: shoji@tokyo-ct.ac.jp (R. Shoji)
Telp:+81-42-6685076, Fax:+81-42-6685099

face area and the addition of materials such as metal oxides. In our previous studies, we reported that macroporous TiO_2 which has various pore sizes was prepared by PMMA-templating method, and the highest activity was shown with possessing the smallest pore size and highest surface area among the various-sized photocatalysts and the addition of MnO_2 onto the porous TiO_2 accelerated the photocatalytic oxidation of Pb(II) ions [6][7]. However, it is necessary to improve the photocatalytic activity for practical usages such as water treatment.

The objectives of this study are: (1) synthesizing a CeO_2 photocatalyst having a good crystallinity as well as high surface area and (2) investigating auxiliary catalyst or cocatalyst oxides loaded on the CeO_2 to increase the amount of lead ions removed from water. In order to synthesize porous CeO_2 photocatalyst materials, a hard template method was employed by using commercial silica microspheres as a template [8]. Highly structured macroporous materials composed of uniform pore networks of micrometer level have recently been synthesized by the template method and applied into to many researches, such as photonic, optical, and catalytic applications, due to the main features of high surface area and uniform macropore arrangement.

2. Materials and Methods

2.1 Catalyst preparation

Cerium oxide photocatalysts were prepared according to the two methods, i.e. (1) Template method, and (2) Impregnation method [7,8]. In the template method, macroporous cerium oxides were prepared by the template method, using commercial silica microspheres (Sciqas Series, Sakai Chemical Industry Co. Ltd.) as a template material. Firstly, 2.1 g cerium (III) nitrate hexahydrate and 5 g citric acid (Wako Pure Chemical Industries Ltd., 98.0%) were dissolved in a 40 mL of ion-exchanged water. Then, 6 g silica powder of different particle sizes of 0.05-1.0 μm was dispersed in the solution. The resulting suspension was evaporated in a drying oven at 80 °C. The obtained solid precursor was heated at 350 °C for 1 hour and then 900 °C for 5 hours. Heated sample was soaked into a 1 M NaOH solution at 80 °C for 2 days. After the vacuum filtration of suspension, washed with ion exchanged water for several times and dried at 80 °C.

Meanwhile, in the impregnation method, zinc oxide loaded macroporous cerium oxides was prepared by an impregnation method. The macroporous CeO_2 prepared by the above-mentioned procedure was were impregnated in an aqueous solution 10 wt% of zinc chloride (Wako Pure Chemical Industries Ltd., 98.0%). After the evaporation of water, the obtained sample was heated at 900 °C for 5 hours again.

2.2 Catalyst characterization

Sample properties were examined by several analytical instruments. Phase identification of the prepared samples were was made by an X-ray diffractometer with Cu-Kα radiation operated at 40 kV and 40 mA (XRD, D8ADVANCE, Bruker AXS). Diffraction intensities were recorded from 20° to 80° at the rate of 2.00 °/min with a 0.02° step. BET surface area of the porous sample was measured by nitrogen adsorption experiments (Flowsorb III, Shimadzu Corporation). After the heat pretreatment of the sample at 120 °C for 30 minutes under the flow of $30\%N_2/70\%Ar$ mixture, the adsorbed amount of nitrogen on the sample was measured at liquid nitrogen temperature. The prepared samples were observed by a scanning electron microscopy (SEM, Quanta 250 SEM, FEI Corporation). The pore distribution was also measured by nitrogen adsorption experiments (BELSORP-mini II, BEL Japan).

2.3 Activity test

Photocatalytic experiments were carried out in a batch reactor. Firstly, 10 mL of 2.4 mmol/L solution of Pb(II) ion and 30 mg of the photocatalyst were put together in a 50 mL beaker, and then UV LED light (NICHIA Corporation, NCSU033B, 15 mW/cm^2, 365 nm) was irradiated to the suspension. After every experiments, 10 mL of the solution was sampled and filtered continuously at every measurements. At the same time, pH of the solution was continuously measured. Pb(II) and Zn(II) ions in the filtrate were analyzed by an inductively coupled plasma atomic emission spectroscopy (ICP-AES, ICP-7510, SHIMADZU). The adsorption rate equation was fitted by Equation (1).

$$n_a = n_m \times (1\text{-exp } (-a \times t)) \quad (1)$$

where n_a is the maximum amount of adsorption, n_m is the amount of adsorption, a is constant number, and t is reaction time. The photocatalytic activity was showen by the lead ion removal amount with UV irradiation minus the lead ion removal amount without UV irradiation.

3. Results and Discussion

3.1 Macroporous CeO_2 loaded with ZnO

Figure 1 shows the BET surface area of the macroporous CeO_2 prepared with various sizes of silica spheres (0.05-0.4 μm). The BET surface area tended to increase in accordance with the decrease in the particle size of the silica used, and the highest BET surface area of 73.8 m^2/g was given in the sample prepared with the smallest silica sphere (0.05 μm). The curve is ideally expected to be a quadratic curve, in which the particle size of silica was proportional to the BET surface area, due to the non uniform silica template. In the case of using 0.4 μm of sphere for template, the BET surface area of the macroporous TiO_2 was larger than the macroporous CeO_2. In the case of using less than 0.15 μm of sphere, the final maximum BET surface area of the macroporous CeO_2 (73.8 m^2/g) was larger than the macroporous TiO_2 (57.6 m^2/g). The macroporous CeO_2 which has a high BET surface area was synthesized because the BET surface area of commercial CeO_2 nano particles shows 10-30 m^2/g [9]. Moreover, since the theoretical BET surface area of the macroporous CeO_2 using 0.05 μm of silica is 86.3 m^2/g, it can be concluded that macroporous CeO_2 were successfully synthesized.

Figure 2 shows a SEM image of the synthesized macroporous CeO_2 (using 0.05 μm silica). Many pores having about 0.05 μm of pore size were observed as many black spots in the SEM image. They were formed by eluting silica spheres from the macroporous CeO_2 precursor. Comparing our synthesized macroporous TiO_2, the arrangement of pores in the macroporous CeO_2 was not uniform. In the preparation of template, silica was settled by sedimentation. Since the silica precipitation at the bottom of the solution was not so apparent, the silica template is easily broken. Taking the SEM observation and BET surface area measurement together into consideration, the CeO_2 having many pores was synthesized. Figure 3(a) shows nitrogen adsorption isotherms of macroporous CeO_2 prepared by using 0.05 μm silica. The observed hysteresis indicates the existence of macro pores. Figure 3 (b) and (c) shows the pore size distribution calculated by BJH theory. The distribution obtained from the adsorption isotherm indicates that main pore size could be more than 20 nm. Considering that silica spheres used as a template was 0.05 μm, the prepared macroporous CeO_2 could have macro pores of 20-50 nm on average. On the other hand, the size distribution with a peak top at 12 nm was observed from the desorption isotherm. Since the bottle neck pore size of pore network can be given by the distribution, it is speculated that the macroporous CeO_2 probably have a macroporous structure composed of 20-50 nm macropores connected by average 12 nm small pores.

Figure 4 (a) indicates the XRD pattern of the macroporous CeO_2 prepared with silica spheres (0.4 μm), where clear sharp peaks were

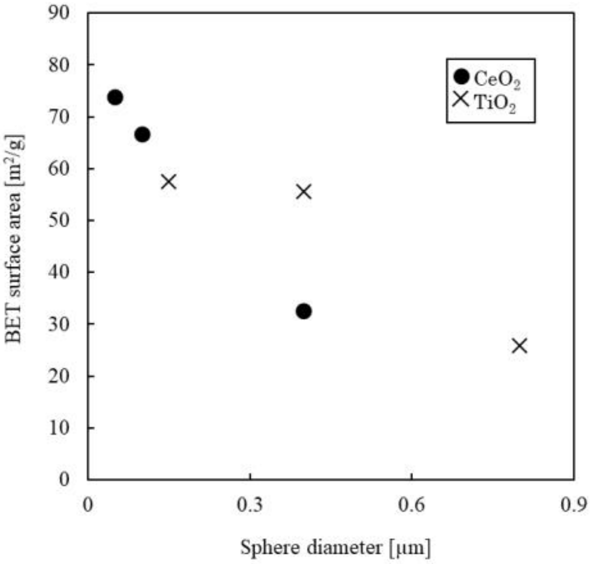

Figure 1. BET surface area of macroporous CeO_2 and TiO_2 [6] prepared with various sizes of Si silica spheres (0.05-0.7 μm), BET surface area of nonporous CeO_2 was 2.0 m^2/g

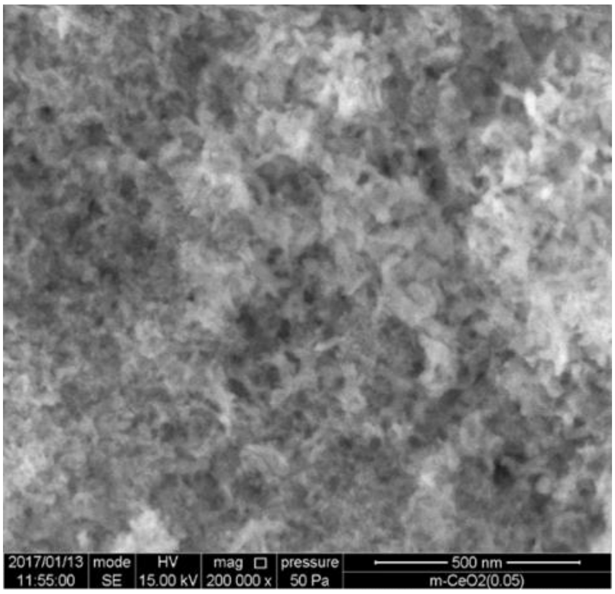

Figure 2. SEM image of the synthesized macroporous CeO_2 (using 0.05 μm silica sphere)

observed corresponding to the CeO_2 phase. In the XRD pattern shown in Figure 2 (b), clear peaks ascribing to the ZnO phase were observed in the ZnO-loaded sample, which indicates that ZnO particles were fixed on the porous CeO_2 photocatalyst. This XRD pattern shows a similar pattern with ZnO/CeO_2 synthesized by Li *et al.* [10]. It was confirmed that the oxides of ZnO and CeO_2 was successfully formed.

3.2 Removal of lead ions

Figure 5 shows the adsorbed amount of lead ions by the macroporous CeO_2 which have various BET surface areas. The amount of lead ions removal tended to increase in accordance with the increase in the BET surface area. Since the amount of removed lead ions removal was proportional to the BET surface area, the adsorption of lead ions is suggested to be single layer adsorption. Since the order also follows the increasing in the BET surface area, macroporous structure could work effectively for an improvement of the removal of lead ions. The BET surface area of the macroporous CeO_2 was larger or similar in size to the macroporous TiO_2 which was synthesized by our previous study [6].

Figure 6 indicates the amount of removed lead ions by the ZnO loaded macroporous CeO_2 against reaction time. The adsorption rate can be formulated with the Langmuir adsorption model. In addition, since the amount of lead ions removal is proportional to the BET surface area (Figure 4), the adsorption rate is suggested to be a single layer adsorption. Comparing commercial adsorbent like an activated carbon (q_m = 0.050 mg/g), the ZnO loaded macroporous CeO_2 also showed a high performance as an adsorbent (q_m = 0.29 mg/g) [11]. The photocatalytic removal started after 60 min of

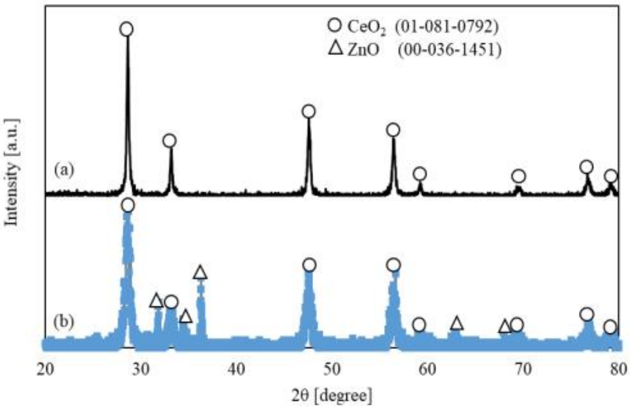

Figure 4. XRD pattern of photocatalysts: (a) macroporous CeO_2 prepared with 0.4 µm silica spheres, (b) 50 wt% $ZnO/m\text{-}CeO_2$

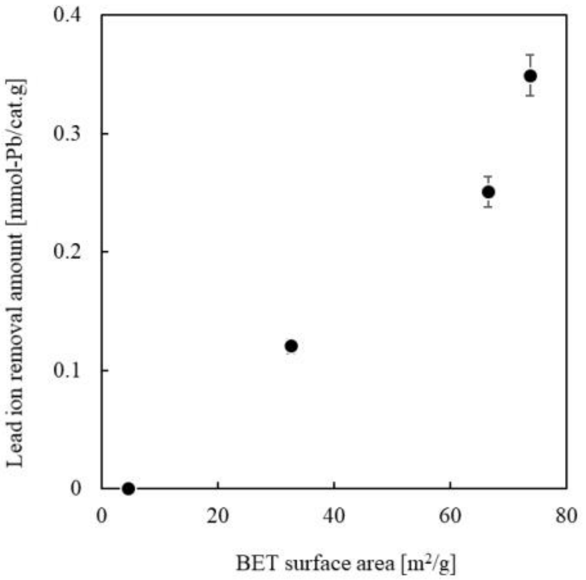

Figure 5. Amount of lead ions removed by the macroporous CeO_2 which have various BET surface areas

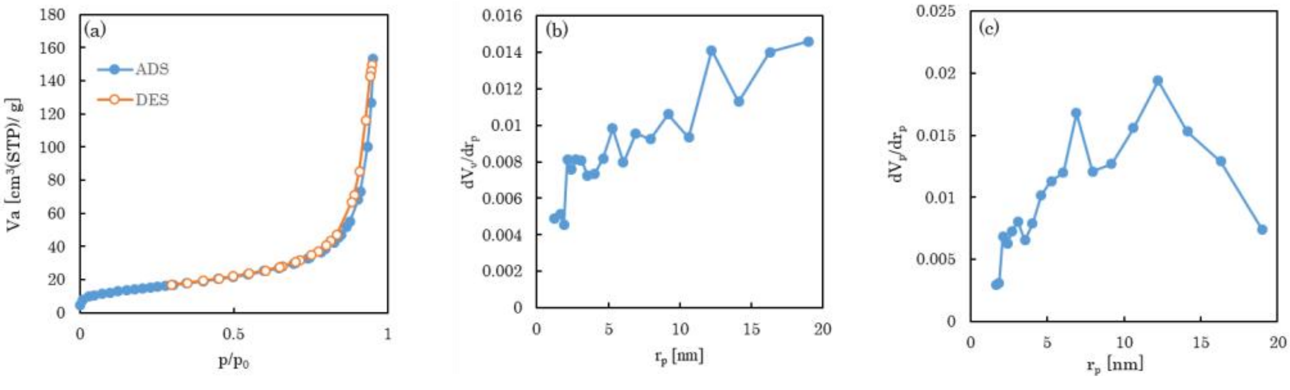

Figure 3. The nitrogen adsorption-desorption measurement of macroporous CeO_2 (using 0.05 µm silica sphere) (a) nitrogen adsorption isotherms, (b) BJH plots of adsorption, (c) BJH plots of desorption

the reaction time and increased with the time. In the process of the removal of lead ions, zinc ions were dissolved at the same time. Throughout the experiment, the pH of the solution was almost constant (5.2±0.2). Since the photocatalytic activity was sufficiently identified for 3 hr, the performance of each photcatalyst was compared after 3 h as shown in Figure 7.

Neither the ZnO only nor the macroporous CeO_2 showed an appreciable photocatalytic activity. However, comparing between the macroporous CeO_2 only and the ZnO loaded on macroporous CeO_2, the ZnO loaded macroporous CeO_2 had a larger photocatalytic activity. Since the ZnO gave a larger amount of removed lead ions, the loading of ZnO was effective for removing lead ions from water. Moreover, the ZnO loaded macroporous CeO_2 showed a larger amount of removed lead ions than that using the non porous CeO_2. It is assumed that the increase in the lead ion removal by the macroporous CeO_2 was caused by an improved adsorption capacity due to the high BET surface area. Moreover, according to a previous study [12], electron-hole recombination on the CeO_2 surface was inhibited because the photogenerated electrons from CeO_2 are transferred to the ZnO. That is why the photocatalytic activity of the macroporous CeO_2 with ZnO was increased compared to that of CeO_2 only. Comparing an our previous study [7], the ZnO loaded macroporous CeO_2 shows higher performance for removing lead ions than TiO_2 photocatalysts, though the BET surface area of them are almost same.

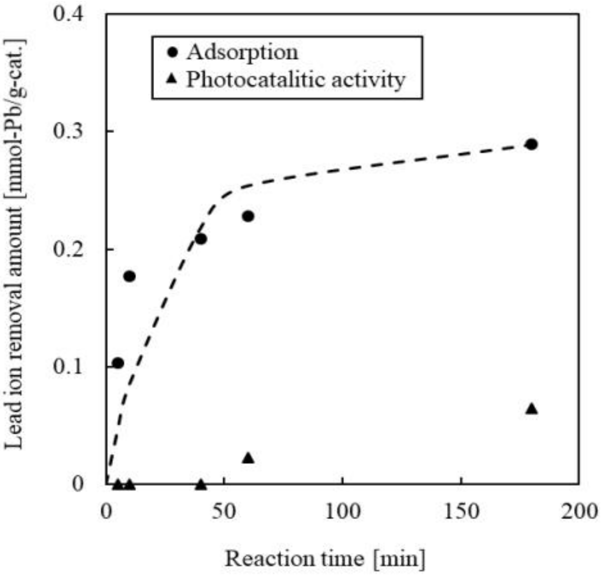

Figure 6. Amount of lead ions removed by ZnO loaded macroporous CeO_2 against reaction time. Dashed carve means Langmuir plots

Figure 8 shows the amount of zinc ions dissolved against the amount of removed lead ions. The amount of dissolved zinc ions from the photocatalysts was increased in accordance with increase in the amount of removed lead ions. The redox potential of Zn (-0.7626 V) is lower than that of Pb (-0.1263 V). The ionization tendency of Zn^{2+} is stronger than that of Pb^{2+}. In addition, it has been reported that ZnO is oxidized to Zn^{2+} by the photogenerated holes [13]. Since 1 mol of zinc ions was dissolved for

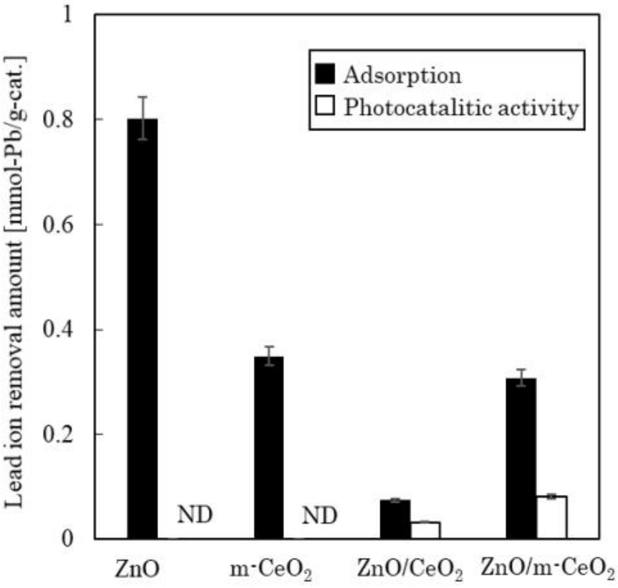

Figure 7. Amount of lead ions removed by ZnO/CeO_2 (reaction time: 3 h). ND: No photocatalytic activity was detected

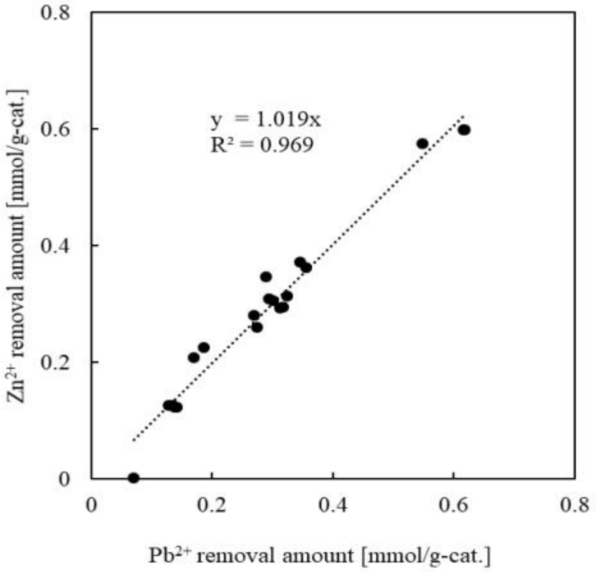

Figure 8. Plots of the amount of zinc ions dissolved against the amount of lead ions removed by ZnO loaded macroporous CeO_2

1 mol of removed lead ions, this reaction is possibly caused by the ion-exchange reaction between lead ions and zinc ions, which is promoted by the light irradiation.

In this study, the photocatalytic activity was increased by the ZnO loaded on the CeO_2. However, Ayawanna *et al.* reported that lead ions were removed by the Gd_2O_3 loaded on the CeO_2 which was calcined at 1400 °C without dissolved dissolution of Gd^{3+} ions into water [5]. In order to improve the macroporous CeO_2 photocatalyst with ZnO prepared in this study, the elution of zinc ions should be decreased by high temperature calcination.

4. Conclusions

Removal of Pb(II) ions from water was performed by the coupling method of adsorption and photocatalysis over the porous CeO_2 loaded with ZnO. Using commercial silica microspheres having various sizes, macroporous CeO_2 photocatalysts were successfully fabricated by the template method and, the largest BET surface area of the macroporous CeO_2 photocatalyst was 73.6 m^2/g. The addition of ZnO showed a larger amount of removed lead ions. The addition of ZnO for the macroporous CeO_2 shows a larger amount of removed lead ions than the non porous CeO_2. In the case of removal of lead ions, since 1 mol of zinc ions was dissolved for 1 mol of removed lead ion, it was suggested that this reaction is the ion-exchange reaction between lead and zinc ions and was promoted by the UV light irradiation.

Acknowledgment

This work is supported by a joint research grant from Nagaoka University of Technology. Author can describe any supports here.

References

[1] Fu, F., Wang, Q. (2011). Removal of heavy metal ions from wastewaters: A review. *Journal of Environmental Management,* 92: 407-418.

[2] Barakat, M.A. (2011). New trend in removing heavy metals from industrial wastewater. *Arabian Journal of Chemistry*, 4: 361-377.

[3] Bailey, S.E., Olin, T.J., Bricka, R.M., Adrian, D.D. (1999). A review of potentially low-cost sorbents for heavy metals. *Water Research,* 33: 2469-2479.

[4] Chen, D., Ray, A.D. (2001). Removal of toxic metal ions from wastewater by semiconductor photocatalysis. *Chemical Engineering Science*, 56: 1561-1570.

[5] Ayawanna, J., Teoh, W., Niratisairak, S., Sato, K. (2015). Gadolinia-modified ceria photocatalyst for removal of lead(II) ions from aqueous solutions. *Material Science Semiconductor Processing,* 40: 136-139.

[6] Kobayashi, Y., Nozaki, T., Kanasaki, R., Shoji, R., Sato, K. (2017). Fabrication of Macroporous TiO_2 Loaded with Magnetite for Photocatalytic Degradation of Methylene Blue. Journal Chemical Engineering of Japan, 50: 132-135.

[7] Kobayashi, Y., Nozaki, T., Kanasaki, R., Shoji, R., Sato, K. (2017). Improving Effect of MnO_2 Addition on TiO_2-Photocatalytic Removal of Lead Ion from Water. Journal of Water and Environment Technology, 15: 35-42.

[8] Yoshida, M., Hamanaka, M., Dong, Q., Yin, S., Sato, T. (2015). Synthesis of morphology controlled SnO_2 and its oxygen storage capacity. Journal of Alloys and Compounds, 646: 271-276.

[9] Deng, X., Cheng, J., Hu, X., Wang, L., Li, D., Gao, K. (2017). Biological effects of TiO_2 and CeO_2 nanoparticles on the growth, photocsynthetic activity, and cellular components of marine diatom Phaeodactylum tricornutum. *Science of the Total Environment,* 575: 87-96.

[10] Li, C., Zhang, X., Dong, W., Liu, Y. (2012). High photocatalytic activity material based on high porosity ZnO/CeO_2 nanofibers. *Materials Letters,* 80: 145-147.

[11] Asuquo, E., Martin, A., Nzerem, P., Siperstein, F., Fan, X. (2017). Adsorption of Cd(II) and Pb(II) ions from aqueous solutions using mesoporous activated carbon adsorbent: quilibrium, kinetics and characterisation studies. Journal of Environment Chemical Engineering, 5: 679-698.

[12] Lamba, R., Umar, A., Mehta, S.K., Kansal, S.K. (2015). CeO_2-ZnO hexagonal nanodisks: Efficient material for the degradation of direct blue 15 dye and its simulated dye bath effluent under solar light. *Journal of Alloys and Compounds,* 620: 67-73.

[13] Mohammadi, Z., Sharifnia, S., Shavisi, Y. (2016). Photocatalytic degradation of aqueous ammonia by using TiO_2-ZnO/LECA hybrid photocatalyst. *Materials Chemistry and Physics,* 184: 110-117.